

## Inelastic neutron scattering from single crystal Zn under high pressure

J. G. Morgan

*Manuel Lujan Jr. Neutron Scattering Center, Los Alamos National Laboratory, Los Alamos, New Mexico 87545  
and Department of Physics, Box 3-D, New Mexico State University, Las Cruces, New Mexico 88003*

R. B. Von Dreele

*Manuel Lujan Jr. Neutron Scattering Center, Los Alamos National Laboratory, Los Alamos, New Mexico 87545*

P. Wochner and S. M. Shapiro

*Department of Physics, Brookhaven National Laboratory, Upton, New York 11973*

(Received 29 January 1996)

Inelastic neutron-scattering experiments have been performed for single crystals of Zn under pressures up to 8.8 GPa at 300 K. The phonon modes  $q/q_{\max} = \xi = 0.075$  and  $\xi = 0.10$  were measured in the transverse acoustic branch  $\Sigma_3$ , where  $q=0$  corresponds with the elastic constant  $C_{44}$ . The phonon energy showed a substantial hardening with increasing pressure. The experimental data below 6.8 GPa for  $\xi=0.075$  yield a constant Grüneisen mode  $\gamma_i = -\ln\omega_i/\ln V$  of 2.25 in good agreement with a previous calculation [H. Ledbetter, *Phys. Status Solidi B* **181**, 81 (1994)]. Above 6.8 GPa, there is a very rapid increase of  $\gamma_i$  which is indicative of the presence of a giant Kohn anomaly. This rapid divergence at high pressure indicates that a phonon softening may occur at pressures higher than 8.8 GPa caused by the collapse of the giant Kohn anomaly via an electronic topological transition (ETT). In an earlier Mössbauer Zn study at 4 K [W. Potzel *et al.*, *Phys. Rev. Lett.* **74**, 1139 (1994)], a drastic drop of the Lamb-Mössbauer factor was observed at 6.6 GPa, which was interpreted as being due to phonon softening, indicating this ETT had occurred. This paper also compares the compressibility data for single crystal Zn and Zn powder using neutron scattering. The results were found to be similar to an earlier x-ray Zn powder experiment [O. Schulte *et al.*, *High Pressure Res.* **6**, 169 (1991)]. [S0163-1829(96)03225-0]

### I. INTRODUCTION

For many years the hexagonal close-packed (hcp) structure of nontransition metallic Zn and Cd have been intensively investigated, since the axial  $c/a$  ratios of 1.856 for Zn and 1.89 for Cd are much greater than the ideal ratio,  $c/a = \sqrt{8/3} = 1.633$ . Because of this large  $c/a$  ratio, many solid-state properties of Zn and Cd are highly anisotropic.<sup>1-13</sup> From numerous theoretical and experimental studies of Zn, it is clear that the electronic structure of Zn plays a particularly important role in the manifestation of these properties. The asymmetry of the electronic charge distribution caused by the  $p$ -band mixing is the origin of the large  $c/a$  ratio for Zn.<sup>14</sup> As a consequence, the Fermi surfaces of Zn and Cd differ from those in a normal hcp structure, and this difference leads to the presence of the giant Kohn anomaly. When the Fermi level lies inside the energy gap corresponding with a certain reciprocal-lattice vector  $\mathbf{G}(hkl)$ , so that  $2|\mathbf{k}_F| = |\mathbf{G}(hkl)|$  is satisfied, a giant Kohn anomaly appears at  $\mathbf{q} \approx 0$ , in the long-wavelength region. Unlike the normal Kohn anomaly, the giant Kohn anomaly can change the acoustic sound velocity substantially, and therefore low-acoustic phonon energies are strongly affected.<sup>15</sup> In the case of Zn or Cd, the Fermi level is located at the symmetry point  $L$  corresponding with  $\mathbf{G}(101)$  in the local band gap and results in a giant Kohn anomaly. Consequently, the Fermi surface “butterflies” at  $L$  are suppressed in the third Brillouin zone, and no electronic states exist at  $L$ . The giant

Kohn anomaly has been observed by Chernyshov *et al.* in Cd.<sup>16</sup>

High-pressure experiments on Zn and Cd are of particular interest because of the anisotropic compressibility of these metals.<sup>3</sup> Under high pressure, the  $c$  axis is much more compressed than the  $a$  axis, and therefore the  $c/a$  ratio decreases towards the ideal ratio, and the structures of Zn and Cd become less anisotropic, and one would expect that changes in the Fermi surface will occur with the decreasing  $c/a$  ratio. Several high-pressure experiments employing Mössbauer spectra and the de Haas-van Alphen (dHvA) method for Zn and Cd have been reported during the last decade.<sup>4,17,18</sup> An electronic topological transition (ETT), or change of the shape of the Fermi surface, are clearly indicated in the high-pressure dHvA study of Cd.<sup>17</sup>

In a recent low-temperature ( $T=4.2$  K), high-pressure Mössbauer experiment on <sup>67</sup>Zn,<sup>18</sup> it was shown that the Lamb-Mössbauer factor (LMF) drops off sharply at an external pressure of 6.6 GPa. Since the LMF is more sensitive to low-frequency phonons, it has been suggested that softening of the low-frequency acoustic and optical phonons at 6.6 GPa is the reason for the sudden decrease in the LMF, and that a collapse of the giant Kohn anomaly is responsible for this phonon softening. From the linearized augmented plane-wave calculations<sup>18</sup> for Zn, an ETT is anticipated at a volume reduction of  $\Delta V/V_0 = -0.115$ . The phonon softening at 6.6 GPa in the Mössbauer experiment<sup>18</sup> indicates that the ETT has occurred. According to Potzel *et al.*,<sup>18</sup> the ETT destroys the formation of the giant Kohn anomaly on the Fermi

surface and results in a softening of the phonons.

The Mössbauer experiment<sup>18</sup> suggests that the lattice dynamics of Zn are strongly influenced by an ETT at high pressure. Phonon measurements are the most direct probe of lattice dynamics, therefore it is of great interest to measure the low-frequency acoustic phonons of Zn under high pressure to see the effect of a giant Kohn anomaly and determine if an ETT occurs. Until now, exact information about the phonons of Zn under high pressure has not been available because of the difficulties of performing high-pressure neutron inelastic-scattering experiments. We now report a high-pressure neutron inelastic phonon measurements for single crystals of Zn.

Several measurements of the compressibility of Zn powder<sup>19,20</sup> and single crystal Zn (Ref. 21) with pressure have been reported. There are some discrepancies between these measurements, especially in measurements of the change of the  $c/a$  ratio with pressure. It has been suggested that this discrepancy is caused by large deviatoric stresses related to the type of pressure cell and pressure medium.<sup>19</sup> We also report the high-pressure neutron data for the compressibility of both powder and single-crystal Zn.

## II. EXPERIMENTAL

The high-pressure cell used for this experiment was a Paris-Edinburgh (PE) cell.<sup>22</sup> There are two different size anvils available for this PE cell, with diameters of 6 and 8.5 mm and sample volumes of approximately 100 and 300 mm<sup>3</sup>, respectively. The relatively large sample volumes allowed us to perform neutron inelastic-scattering experiments on single crystals under high pressure. In order to obtain a sufficiently intense phonon signal from Zn, we have used large size anvils (300 mm<sup>3</sup> sample volume). The gaskets for the PE cell consist of an outer toroidal gasket and a flat inner washer. In this experiment, we used TIMETAL 21S (Titanium Metals Corporation), a titanium aircraft alloy, as the outer gasket and 51/49 TiZr alloy as the inner washer. Both gaskets allow high neutron penetration with enough mechanical strength to prevent breakage under high stress. In this work we have been able to generate hydrostatic pressures to at least 8.8 GPa with these gaskets using the large volume anvils. The effective sample volume is determined by the thickness of the flat washer, which in our experiments was about 2.2 mm before pressure loading, and about 0.7 mm at a pressure of 8.0 GPa. A single crystal of Zn ( $4 \times 4 \times 3$  mm<sup>3</sup>) and a Pb pressure calibration coil were surrounded by a paste of fluorinert and aerogel (low-density silica). The Zn crystal was aligned in the desired orientation in the assembly of gaskets and anvils with the neutron beam prior to pressure loading.

Neutron inelastic experiments were performed on the triple-axis spectrometer H4S at the High Flux Beam Reactor (HFBR) operating at 30 MW at Brookhaven National Laboratory. Since the sample volume was small, wide collimation was used. Soller collimators of 40', 40', 40', and 80' for inpile, monochromator to sample, sample to analyzer, and analyzer to <sup>3</sup>He detector, respectively, were used to obtain sufficient intensity for these experiments. The energy of the incident neutron beam was fixed at 14.7 meV, using the (002) planes of a vertically focusing pyrolytic graphite (PG)

crystal monochromator and a fixed takeoff angle of 41.1°. PG (002) was also used as the analyzer, and a PG filter was used to eliminate higher-order contamination. Two adjustable slits between the monochromator downstream collimator and the sample were used to confine the incident beam to just the sample region. A 1 cm wide slit in front of the analyzer was used to further reduce background scattering.

The Pb (111) powder-diffraction peak was used to determine the pressure using the known equation of state (EOS) for Pb.<sup>23</sup> The uncertainty of the pressure determination using this method was approximately 0.1 GPa. The Pb (111) peak position remained fixed at the same position at high pressure, even after 30 h of data acquisition, indicating excellent pressure stability. The constant- $Q$  method with fixed incident energy was employed for the phonon measurement. The phonon branch measured in these experiments was the transverse-acoustic mode, in  $\Sigma_3$  with wave vector  $\mathbf{q}$  along (010) and polarization parallel to (001), which is associated with the elastic constant  $C_{44}$  at  $\mathbf{q}=0$ . This branch was measured because it has been shown that the giant Kohn anomaly can modify the elastic constant  $C_{44}$  considerably.<sup>16</sup> To measure this branch, the crystal must be oriented with  $(\bar{1}20)$  perpendicular to the scattering plane. In our experiments, only the  $\xi=0.075$  and  $\xi=0.10$  phonons were measured, where  $\xi$  is the reduced wave vector,  $q/q_{\max}$ , and  $q_{\max}=4\pi/\sqrt{3}a$ . Phonon peaks at  $\xi<0.075$  cannot be resolved from the elastically scattered peak. The phonons for  $\xi>0.10$  were too high in energy to have an appreciable signal for the size of this sample. Moreover, as we are interested in the behavior of  $C_{44}$ , we were only interested in the low- $\xi$  region. The phonon measurements were performed around the Bragg peak (002), which has a strong elastic intensity. Both energy gain and energy loss were used in this experiment, depending on the signal-to-background ratio. Focusing effects were taken into consideration to optimize the resolution of the phonon energy during the measurements. The counting time was 10–35 h for one phonon scan (typically from 1.7 to 5.0 meV in steps of 0.1 meV for  $\xi=0.075$ ) depending on the signal intensity. The  $(\bar{1}20)$  orientation of the crystal allowed us to determine both lattice parameters  $a$  and  $c$  of Zn for each pressure giving both the volume compressibility and change in the  $c/a$  ratio. The precision of our determination of the lattice parameters was  $\pm 0.0005$  Å. The results of three separate pressure runs were consistent. The highest pressure achieved for the measurement of the phonon frequency in these experiments was 8.8 GPa.

High-pressure Zn powder neutron-diffraction experiments were performed on the high intensity powder diffractometer at the Manuel Lujan Jr. Neutron Scattering Center at Los Alamos National Laboratory to obtain powder compressibility data for comparison to the single-crystal data. The same PE cell and gaskets used in the inelastic-scattering experiment were also used for the powder-diffraction experiments. The 100 mm<sup>3</sup> volume anvils were used for the powder experiments. Two powder runs with different geometries for data collection were carried out. In one setup (horizontal), the hydraulic force was parallel to the beam, and in the other (vertical) setup, the hydraulic force was perpendicular to the beam. The latter configuration was the same geometry used in the phonon experiment. The EOS of NaCl was used to

calibrate the pressure<sup>24</sup> in the Zn powder experiments. The diffraction patterns of Zn and NaCl were collected by time-of-flight spectroscopy at  $2\theta=90^\circ$  for both powder experiments. Typical data collection times were 7 h for the horizontal setup and much shorter (4 h) for the vertical setup due to much lower neutron absorption and improved detector solid angle. The pressure achieved for the horizontal set up was 5.4 GPa, and 7.8 GPa for the vertical configuration. Both experiments were limited by gasket failures at high pressure caused by the lubrication of the surfaces between the gaskets and the anvils by the Zn sample.

### III. RESULTS

The mosaic spread of the single-crystal Zn (17' at ambient pressure) increased rapidly with increasing pressure at low pressure, but was relatively constant at higher pressure (>3.0 GPa). The relationship between the mosaic spread and pressure indicated that much better hydrostatic conditions existed at higher pressure, as is typical for the PE high-pressure cell.

The axial compressibilities measured during these experiments give the  $c/a$  ratio vs pressure curve shown in Fig. 1. Both the  $a$  and the  $c$  lattice parameters measured from the high-pressure single-crystal Zn experiments were fitted by the Murnaghan equation,

$$\frac{r}{r_0} = \left[ \left( \frac{\beta'}{\beta_0} \right) P + 1 \right]^{-1/\beta'}, \quad (1)$$

where  $r/r_0$  is either the  $a$  or  $c$  lattice parameter,  $\beta_0^{-1} = -(d/dP)(\ln r)|_{P=0}$  is the linear compressibility, and  $\beta'$  is the pressure derivative of  $\beta$ . The parameters  $\beta_0$  and  $\beta'$  are listed in Table I. From Table I, one obtains the ratio of the linear compressibility.  $\beta_0(a)/\beta_0(c) = 7.94$ , showing the large anisotropy of Zn. Thus, the  $c$  lattice parameter is much more compressible than  $a$ . As a result, the value of the  $c/a$  ratio decreases towards the ideal value,  $\sqrt{8/3}$ , with the increasing pressure as shown in Fig. 1. The  $a$  lattice parameter and  $c$  lattice parameter versus the relative volume  $V/V_0$  are shown in Fig. 2, and the  $c/a$  ratio versus  $V/V_0$  is plotted in Fig. 3. In our work, the  $c/a$  ratio (Fig. 3) decreased monotonically with decreasing  $V/V_0$  in contrast with the results of Lynch and Drickamer.<sup>20</sup> For comparison, the two powder data sets with different PE cell orientation are also shown in Figs. 2 and 3. The lattice parameters of Zn and NaCl were obtained by Rietveld refinement using the general structure analysis system.<sup>25</sup> The pressure was determined from the known EOS of NaCl.<sup>24</sup> We have noticed slight differences in the  $c/a$  ratio among the three data sets, and a slightly negative curvature in one powder data set that was obtained from the horizontal setup (see Fig. 3), otherwise, all the EOS data (single crystal and powders) are quite similar.

Figure 4 shows the volume compressibility of Zn measured in the single-crystal experiments. The experimental data are fitted to the Birch equation,

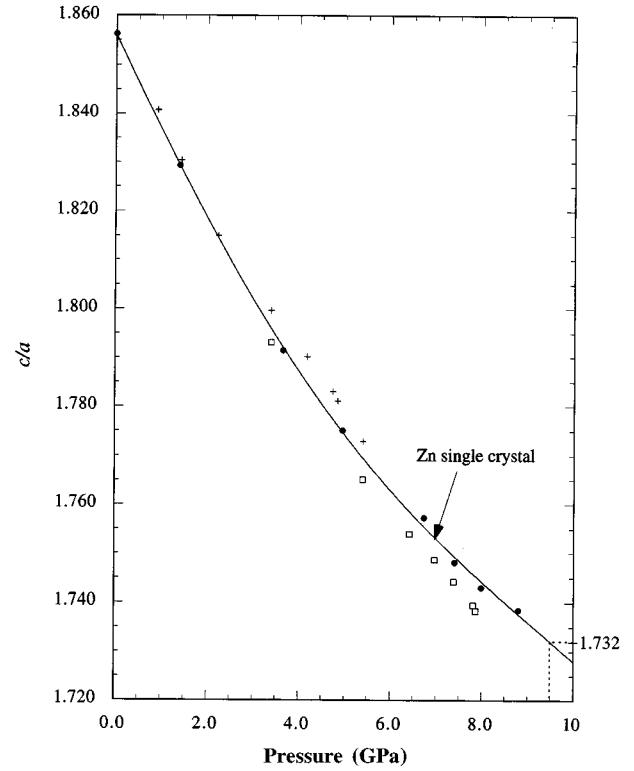


FIG. 1. The  $c/a$  ratio of Zn versus pressure. The closed-circles and fitting curve represent the single-crystal data, the open-squares represent the powder data in the vertical setup, and the crosses represent the powder data in the horizontal setup, in this figure and subsequent figures.

$$P = \frac{3}{2} K_0 \left\{ \left( \frac{V}{V_0} \right)^{-7/3} - \left( \frac{V}{V_0} \right)^{-5/3} \right\} \left[ 1 - \frac{3}{4} (4 - K') \right] \times \left\{ \left( \frac{V}{V_0} \right)^{-2/3} - 1 \right\}, \quad (2)$$

to give the bulk modulus  $K_0 = 57 \pm 2$  GPa, which is quite close to the value of 56 GPa reported from an x-ray powder experiment.<sup>19</sup> The pressure derivative  $K'$  obtained in this work is  $7.4 \pm 0.7$  for the single crystal Zn. There is very little difference between the single-crystal data and two powder sets, which shows that the pressure calibration using Pb and NaCl are very consistent.

Figure 5 shows some examples of the phonon groups at ambient pressure and high pressure. One can see that the phonon peak becomes broader with the increasing pressure, which is caused by the increasing single-crystal mosaic at high pressure. The phonon energies for the wave vectors  $\xi=0.075$  and  $\xi=0.10$  versus  $V/V_0$  are plotted in Fig. 6, and show substantial hardening with increasing pressure. We did not measure the phonon energy at pressures above 7.4 GPa

TABLE I. Linear compressibility for the lattice parameters of Zn.

Lattice parameters	$\beta_0$ (GPa)	$\beta'$
$a$	$566(\pm 32)$	$26(\pm 9)$
$c$	$71(\pm 2)$	$10.4(\pm 0.6)$

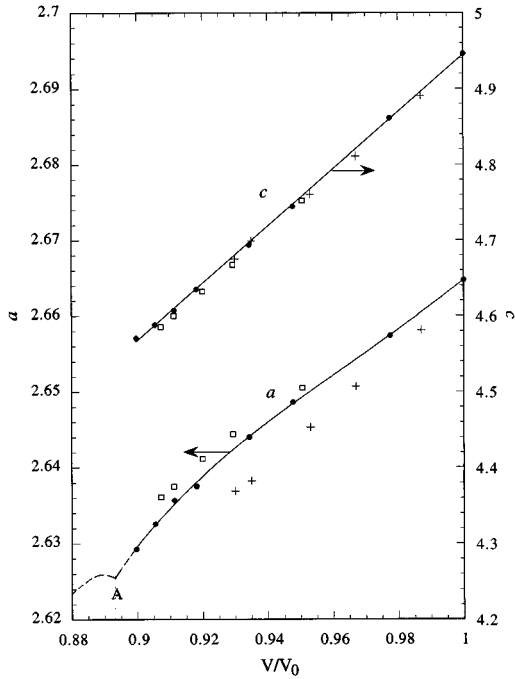


FIG. 2. The lattice parameters  $a$  and  $c$  of Zn versus the relative volume  $V/V_0$ . The fitting curve is only for the single-crystal data. Notice the increment for the  $c$  lattice parameter is ten times greater than the scale for the  $a$  lattice parameter.

for  $\xi=0.1$ , because of the length of time to complete one phonon scan at higher pressure and higher phonon energies. The increasing phonon energy with  $V/V_0$  for  $\xi=0.075$  is quite unusual, while the phonon energies vs  $V/V_0$  for

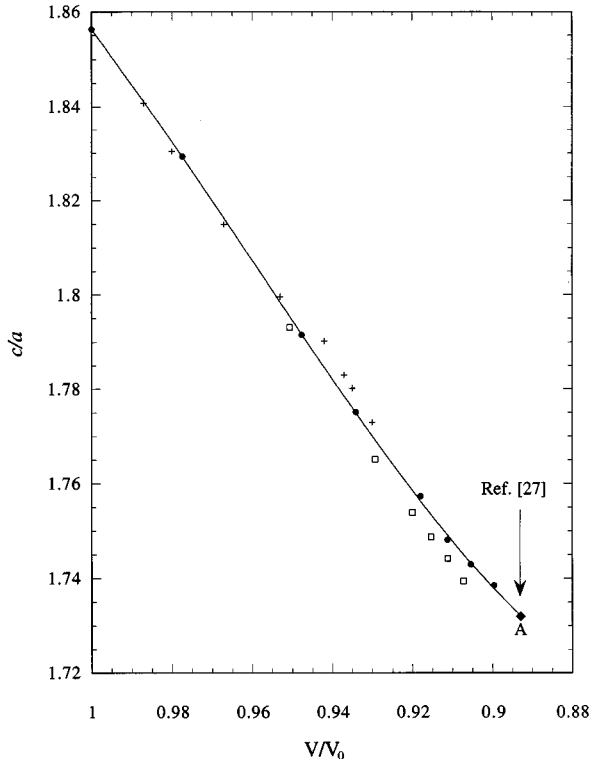


FIG. 3. The  $c/a$  ratio of Zn versus the relative volume  $V/V_0$ . Point A (corresponding with  $V/V_0=0.893$ ,  $c/a=1.732$ ) is from Ref. 27, where the  $c/a$  ratio singularity occurs.

$\xi=0.1$  are nicely fitted by a simple function that yields a constant Grüneisen parameter  $\gamma_{0.1}$  given by

$$E = A \left( \frac{V}{V_0} \right)^{-\gamma_{0.1}}, \quad (3)$$

where  $A=3.359$ , and  $\gamma_{0.1}=2.44$ . An empirical fitting equation for  $\xi=0.075$  for the phonon energy  $E$ , as a function of the volume compressibility  $V/V_0$ , is given by

$$\ln\{E(0.075)\} = A - \gamma_{0.075} \ln\left(\frac{V}{V_0}\right) + B \left\{ \ln\left(\frac{V}{V_0}\right) \right\}^{16}, \quad (4)$$

where  $A=1.0154$ ,  $\gamma_{0.075}=2.25$ , and  $B=2.2 \times 10^{14}$  for the best fit to the data. We did not observe any softening of the TA  $\Sigma_3$  phonon branch arising from the onset of an ETT.

#### IV. DISCUSSION

Based on several theoretical studies of Zn,<sup>18,28–30</sup> the formation of the giant Kohn anomaly in Zn involves the symmetry point  $L$  where the Fermi level is located inside the local band gap. The theoretical study by Kagan, Pushkarev, and Holas<sup>15</sup> predicts that if the Fermi level is located in the upper band, then the giant Kohn anomaly will increase the phonon energy at  $\mathbf{q} \approx 0$ , and *vice versa*. In the case of Zn,  $E_F$  is located in the upper band gap and moves towards the upper band gap edge with compression under high pressure.<sup>18</sup> When  $E_F$  finally moves up to the band gap edge, the ETT occurs, and electronic states exist at the  $L$  point in the third Brillouin zone, which is the same behavior observed in normal hcp metals with ideal  $c/a$  ratios. The giant Kohn anomaly therefore collapses, and the phonons lose the extra hardening that was gained from the initial volume compression.

For a clear picture, we have determined the so-called “mode  $\gamma$ ’s,” (also called the microscopic Grüneisen parameter) defined by

$$\gamma_i(\mathbf{q}) = - \frac{d(\ln\omega_i(\mathbf{q}))}{d(\ln V)}, \quad (5)$$

where  $\omega_i$  is the phonon frequency for a particular mode  $\mathbf{q}$  and branch  $i$ , and  $V$  is the volume. The  $\gamma_i(\mathbf{q})$ ’s express the effect of dilation of the lattice on the frequencies of the various modes. For  $\xi=0.1$ , we have obtained  $\gamma_{\text{TA}\Sigma_3}(0.1)$  from the fitting equation, Eq. (3), which gives a constant  $\gamma_{\text{TA}\Sigma_3}(0.1)=2.44$ . The slopes of the curves for  $\xi=0.075$  and  $\xi=0.1$  in Fig. 6 are the modes  $\gamma_{\text{TA}\Sigma_3}(0.075)$  and  $\gamma_{\text{TA}\Sigma_3}(0.1)$ , respectively. From this figure, one can see that the  $\gamma_{\text{TA}\Sigma_3}(0.075)$  is nearly constant for pressures up to 6.8 GPa. In this low-pressure range, the curve coincides with the slope  $\gamma=2.24$ , which is identical to the bulk Grüneisen parameter for Zn calculated from the thermal-expansion coefficient, the bulk modulus, and the heat capacity.<sup>26</sup> At higher pressures,  $\gamma_{\text{TA}\Sigma_3}(0.075)$  rapidly diverges. At 8.8 GPa with a volume change of 10%,  $\gamma_{\text{TA}\Sigma_3}(0.075)$  is about 10.3, which is almost 4.6 times higher than the low-pressure value of 2.24. Extrapolation of Eq. (4) indicates that  $\gamma_{\text{TA}\Sigma_3}(0.075)$  increases even more rapidly above 8.8 GPa. This rapid divergence of  $\gamma_{\text{TA}\Sigma_3}(0.075)$  is not sustainable and some softening

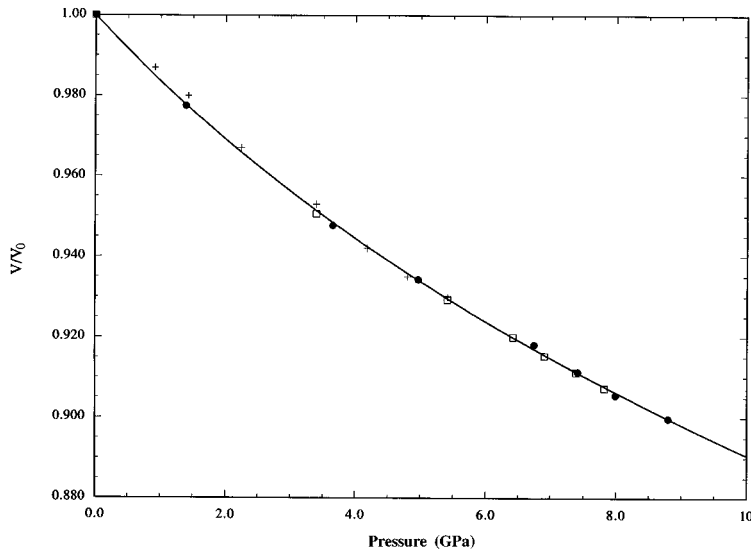


FIG. 4. Volume compressibility of Zn. The Birch equation fitting, Eq. (2), is for the single-crystal experimental data only.

of the phonons will occur at higher pressure, which we anticipate would bring the phonon energies back to the vicinity of the  $\gamma=2.24$  line in Fig. 6. It has been suggested that the increase of the LMF with pressure is an indication of the low-frequency phonon hardening caused by the giant Kohn anomaly.<sup>18</sup> The sharp increase in  $\gamma_{\text{TAS}_3}(0.075)$  in our experimental data is thus due to the giant Kohn anomaly.

In the high-pressure Zn Mössbauer study,<sup>18</sup> a sharp drop of the LMF, which indicates low-energy acoustic-phonon softening, was observed at 6.6 GPa with a volume change  $\Delta V/V_0 = -0.085$ . However, in our inelastic neutron-scattering experiment, phonon softening was not observed, even for pressures up to 8.8 GPa and a volume change  $\Delta V/V_0 = -0.10$ . Our high-pressure Zn phonon measurements have suggested that the ETT can not occur with a

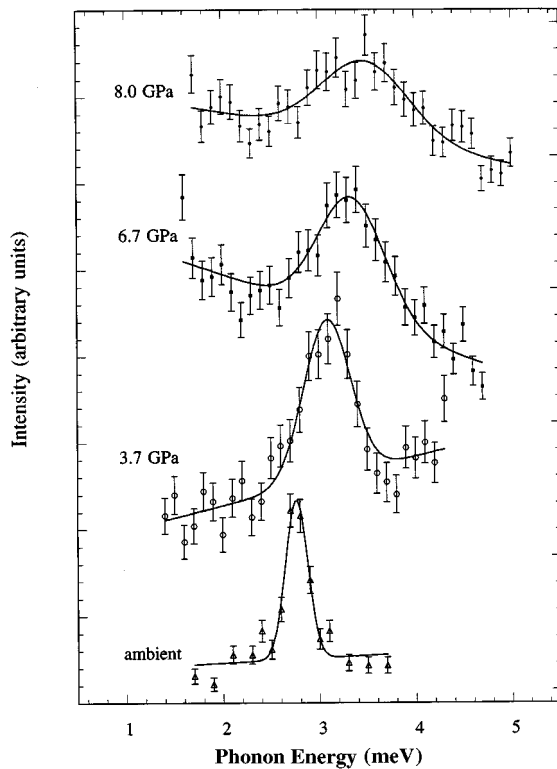


FIG. 5. The phonon groups at pressures 0.0, 3.7, 6.8, and 8.0 GPa. All the peaks were fitted with a Gaussian function to give the peak position corresponding with the phonon energy and a linear function to correct for the background. The peak fitting error was less than 0.06 meV for all the phonon peaks (not shown here) except at 8.8 GPa, which was 0.074 meV. The phonons at ambient pressure and at 3.7 GPa were obtained by the energy loss method, and at 6.8 and 8.0 GPa by the energy gain method.

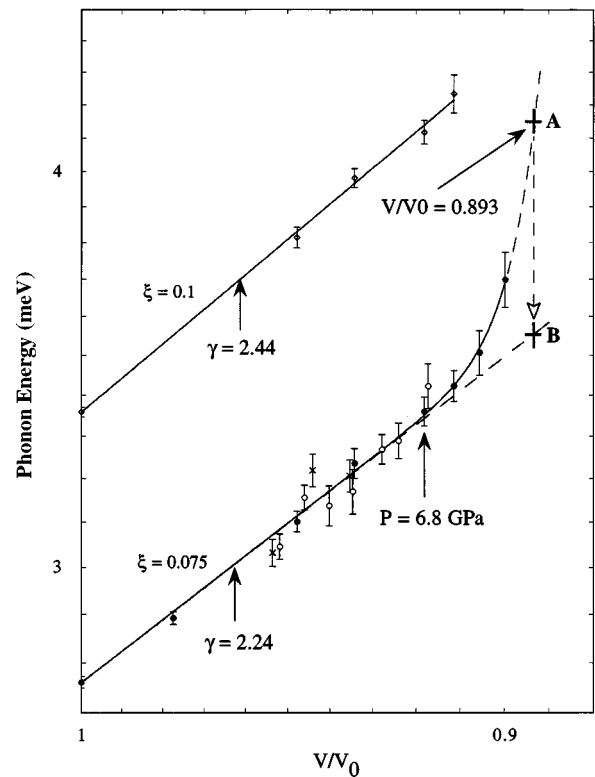


FIG. 6. The measured phonon energies for  $\xi=0.075$  and  $\xi=0.1$  are plotted against the compressed volume  $V/V_0$ . Logarithmic scales are used for both phonon energy  $E$  and compressed volume  $V/V_0$ . The fitting curves used were Eq. (3) for  $\xi=0.1$  and Eq. (4) for  $\xi=0.075$  in the text.  $\bullet$ ,  $\circ$ , and  $\times$  represent three separate experimental runs. The error bars were generated from the Gaussian fit for each measured phonon peak.

volume change less than 10%. The Mössbauer experiment<sup>18</sup> was performed at low temperature,  $T=4.2$  K, where the lattice parameters are smaller than the room temperature values. Also, the thermal-expansion coefficient is anisotropic, making the Zn less anisotropic at low temperature.<sup>1</sup> However, the volume change in the Mössbauer study<sup>18</sup> was calculated using the room-temperature compressibility data.<sup>19</sup> Thus, the actual volume change at 6.6 GPa and  $T=4.2$  K, where the sharp dropoff of the LMF indicated an ETT, is probably greater than 8.5%, as suggested by Kenichi.<sup>27</sup> A band-structure calculation<sup>18</sup> has shown that the ETT should occur at a volume change of 11.5%. In our experiment, the highest pressure was 8.8 GPa with a Zn volume change of 10%, which was apparently insufficient to cause the ETT to occur at room temperature.

On the other hand, several papers<sup>18,20,27</sup> have suggested that a Fermi surface change in Zn might cause an abnormal change in the  $c/a$  ratio. In our Zn single-crystal data, one can see from Fig. 2 that the  $a$  lattice parameter tends to be compressed faster after  $V/V_0=0.92$  so that the  $c/a$  ratio change is less steep, as shown in Fig. 3. Moreover, our phonon data starts to show deviation from a constant Grüneisen parameter  $\gamma=2.24$  (see Fig. 6) at about  $V/V_0=0.92$ . Thus, this slight change in the  $c/a$  ratio could be related to the onset of the giant Kohn anomaly and the pronounced effects on the phonon spectra. In a very recent high-pressure Zn powder x-ray experiment using an angle-dispersive method at room temperature,<sup>27</sup> the volume dependence of the  $c/a$  ratio showed an abnormal change in slope at  $V/V_0=0.893$ , where the  $c/a$  ratio approaches  $\sqrt{3}$  at a pressure of 9.1 GPa. This change is caused by a singularity in the  $a$  lattice parameter at  $V/V_0=0.893$ . This result is consistent with a theoretical calculation<sup>31</sup> that predicted the same change at slightly higher volume,  $V/V_0=0.92$ . It has been suggested that this anomaly in the  $c/a$  ratio is related to the ETT.<sup>27</sup> Comparing our lattice parameter data for single crystal Zn shown in Fig. 2 with the data of Kenichi,<sup>27</sup> we can see that both data sets have exactly the same features in the range of  $0.900 \leq V/V_0 \leq 1$ . The volume dependence of the  $c$  lattice parameter appears to be essentially a straight line, while the  $a$  lattice parameter shows a pronounced fall off at high pressure. In our phonon measurements, the highest pressure was 8.8 GPa, where  $V/V_0=0.900$ , and the  $c/a$  ratio of 1.738 is slightly higher than  $\sqrt{3}$ . The data point  $V/V_0=0.893$ ,  $c/a=\sqrt{3}$  from Ref. 27 is marked in Fig. 3, and our data at

8.8 GPa are quite close to that point. When the  $c/a$  ratio approaches  $\sqrt{3}$ , several Bragg reflection peaks are degenerate, including (002) and (100). In our experiment, the Bragg peaks (002) and (100) are almost degenerate at 8.8 GPa. From Fig. 1 and Eq. (2), the pressure for  $c/a=\sqrt{3}$ , is expected to be about 9.4 to 9.5 GPa. We have also marked  $V/V_0=0.893$  in Fig. 6 as point A. If the ETT occurs at point A, then the phonon energy for  $\xi=0.075$  could show a 0.7 meV drop to the point B where  $\gamma=2.24$ , and the magnitude of this decrease is almost half the total increasing energy change under pressure up to that point. The Mössbauer study<sup>18</sup> has shown a result similar to our conjecture, in which the LMF decreases by a factor of 2 when the ETT occurs.<sup>18</sup> The high-pressure Zn powder x-ray experiment<sup>27</sup> agrees closely with our high-pressure Zn phonon measurements. We therefore strongly suggest that at 300 K the ETT will occur at about 9.4 or 9.5 GPa.

The Zn compressibility data for our single crystal and powder experiments are quite similar. However, we also observed that a notable deviation exists between the powder experiments shown in Figs. 1, 2, and 3. Since these two experiments were carried out with different setup geometries, or different orientations between the incident beam and the applied stress, the two experiments detected different deviatoric stress and therefore gave slightly different results. We therefore believe that the deviatoric stress plays a role in modification of the  $c/a$  ratio of Zn in high-pressure experiments, because Zn is a noncubic anisotropic material and we agree with Schulte, Nikolaenko, and Holzapfel,<sup>19</sup> that the abnormal changes in  $c/a$  ratio observed by Lynch and Drickman are caused by the deviatoric stress due to nonhydrostatic pressure.

#### ACKNOWLEDGMENTS

This work is supported by Manuel Lujan Jr. Neutron Scattering Center, Los Alamos National Laboratory, funded in part by the Office of Basic Energy Sciences Division of Material Sciences of the U.S. Department of Energy (Contract No. W-7405-ENG-36), and High Flux Beam Reactor, Brookhaven National Laboratory, funded in part by the Office of Basic Energy Sciences Division of Material Sciences of the U.S. Department of Energy (Contract No. DE-AC02-76 CH00016). We would also like to thank Uli Wildgruber for his support with the instrumentation and the HFBR technical support team.

<sup>1</sup>W. Potzel, Ulrike Närgler, Th. Obenhuber, J. Zänkert, W. Adlassnig, and G. M. Kalvius, Phys. Lett. **98A**, 295 (1983).

<sup>2</sup>G. Borgonovi, G. Caglioti, and J. J. Antal, Phys. Rev. **132**, 683 (1963).

<sup>3</sup>G. A. Alers and J. R. Neighbours, J. Phys. Chem. Solids **7**, 58 (1958).

<sup>4</sup>W. Potzel, W. Adlassnig, J. Moser, C. Schäfer, M. Steiner, and G. M. Kalvius, Phys. Rev. B **39**, 8236 (1989).

<sup>5</sup>P. Blaha, K. Schwarz, and P. H. Dederichs, Phys. Rev. B **37**, 2792 (1988).

<sup>6</sup>L. Almqvist and R. Stedman, J. Phys. F **1**, 785 (1971).

<sup>7</sup>R. P. Bajpai, J. Phys. F **3**, 709 (1973).

<sup>8</sup>H. F. Bezdek and Leonard Finegold, Phys. Rev. B **4**, 1390 (1971).

<sup>9</sup>G. Caglioti, G. Rizzi, and G. Cubiotti, Solid State Commun. **8**, 367 (1970).

<sup>10</sup>D. L. McDonald, M. M. Elcombe, and A. W. Pryor, J. Phys. C **2**, 1857 (1969).

<sup>11</sup>N. J. Chesser and J. D. Axe, Phys. Rev. B **9**, 4060 (1974).

<sup>12</sup>A. J. Millington and G. L. Squires, J. Phys. C **2**, 2366 (1969).

<sup>13</sup>L. J. Raubenheimer and G. Gilat, Phys. Rev. **157**, 586 (1967).

<sup>14</sup>E. Bodenstedt, B. Perscheid, and S. Nagel, Z. Phys. B **63**, 9 (1986).

<sup>15</sup>Yu. Kagan, V. V. Pushkarev, and A. Holas, Sov. Phys. JETP **57**, 870 (1983).

- <sup>16</sup>A. A. Chernyshov, V. V. Pushkarev, A. Yu Romyantsev, B. Dörner, and R. Pynn, *J. Phys. F* **9**, 1983 (1979).
- <sup>17</sup>S. L. Bud'ko, A. N. Voronovskii, A. G. Gapotchenko, and E. S. Itskevich, *Sov. Phys. JETP* **59**, 454 (1984).
- <sup>18</sup>W. Potzel, M. Karzel, W. Schiessl, M. Köfferlein, and G. M. Kalvius, *Phys. Rev. Lett.* **74**, 1139 (1995).
- <sup>19</sup>O. Schulte, A. Nikolaenko, and W. B. Holzapfel, *High Pressure Res.* **6**, 169 (1991).
- <sup>20</sup>R. W. Lynch and H. G. Drickamer, *J. Phys. Chem. Solids* **26**, 63 (1965).
- <sup>21</sup>Noël Dahan, Jack Bouyroux, René Couty, and André Berthault, *High Pressure Res.* **7**, 225 (1991).
- <sup>22</sup>J. M. Besson, G. Hamel, T. Grima, R. J. Nelmes, J. S. Loveday, S. Hull, and D. Hausermann, *High Pressure Res.* **8**, 625 (1992).
- <sup>23</sup>R. A. Miller, D. E. Schuele, *J. Phys. Chem. Solids* **30**, 589 (1969).
- <sup>24</sup>D. L. Decker, *J. Appl. Phys.* **42**, 3239 (1971).
- <sup>25</sup>A.C. Larson and R. B. Von Dreele, "GSAS—General Structure Analysis System," Los Alamos National Laboratory Report No. LA-UR 86-748, 1986.
- <sup>26</sup>H. Ledbetter, *Phys. Status Solidi B* **181**, 81 (1994).
- <sup>27</sup>Takemura Kenichi, *Phys. Rev. Lett.* **75**, 1807 (1995).
- <sup>28</sup>B. R. Watts and J. Mayers, *J. Phys. F* **9**, 1565 (1979).
- <sup>29</sup>D. Singh and D. A. Papaconstantopoulos, *Phys. Rev. B* **42**, 8885 (1990).
- <sup>30</sup>S. Daniuk, T. Jarlborg, G. Kontrym-Sznajd, J. Majsnerowski, and Stachowiak, *J. Phys.* **1**, 8397 (1989).
- <sup>31</sup>S. Meenakshi, V. Vijayakumar, B. K. Godwal, and S. K. Sikka, *Phys. B* **46**, 14 359 (1992).